AERODYNAMIC AND STRUCTURAL ANALYSIS OF COMPOSITE BLENDED WINGLETS FOR ALUDRA-EE UAV

Qiao Ying Lam, Haris Ahmad Israr*, Shabudin Mat, Mohd Nazri Nasir

Faculty of Mechanical Engineering, Universiti Teknologi Malaysia, 81310 UTM Johor Bahru, Johor, Malaysia

Article history
Received
11th May 2026
Received in revised form
16th June 2026
Accepted
16th June 2026
Published
20th June 2026

*Corresponding author
harisahmad@utm.my

ABSTRACT

Unmanned Aerial Vehicles (UAVs) commonly experience induced drag generated by wingtip vortices, which negatively affects aerodynamic efficiency and endurance. This study investigates the aerodynamic and structural performance of blended composite winglets for the ALUDRA-EE UAV using Computational Fluid Dynamics (CFD) and finite element analysis. Three winglet cant angle configurations (0°, 45°, and 60°) based on the RONCZ 1046 airfoil were evaluated using ANSYS Fluent to analyse lift, drag, lift-to-drag ratio, and vortex intensity. The aerodynamic results showed that the 60° blended winglet produced the best overall performance, achieving the highest lift-to-drag ratio of 22.23 and the lowest vortex intensity among all configurations. The optimized winglet configuration improved UAV range and endurance by approximately 26.14% and 41.7%, respectively. Structural analyses were subsequently conducted using Abaqus to evaluate hollow and solid composite winglet designs with different composite material configurations and ply orientations. The solid winglet constructed using standard carbon fibre fabric demonstrated the lowest displacement and failure indices while maintaining acceptable structural integrity under aerodynamic loading. The findings indicate that the proposed 60° composite blended winglet can significantly enhance the aerodynamic efficiency and structural performance of the ALUDRA-EE UAV.

KEYWORDS

Aerodynamics; CFD; blended winglet; cant angle; composite

INTRODUCTION

Unmanned Aerial Vehicles (UAVs) have gained significant attention in both civilian and military sectors due to their ability to perform surveillance, mapping, environmental monitoring, agricultural inspection, and reconnaissance missions with reduced operational costs and risks to human operators. The aerodynamic efficiency of UAVs plays a key role in determining their flight endurance, range, payload capacity, and fuel or energy consumption. Among the various aerodynamic losses experienced by aircraft and UAVs, induced drag from wingtip vortices is a major contributor to overall flight performance.

Wingtip vortices are formed due to the pressure difference between the lower and upper surfaces of a wing [1]. The high-pressure airflow beneath the wing tends to move towards the low-pressure region above the wing near the wingtip, creating swirling airflow structures known as vortices. These vortices increase induced drag and reduce aerodynamic efficiency. To mitigate this phenomenon, winglets are commonly installed at the wingtip to weaken vortex formation and improve lift distribution. Since the pioneering work of Whitcomb [2], winglets have been widely implemented on modern aircraft to improve lift-to-drag ratio, reduce fuel consumption, and enhance flight stability.

Various winglet configurations have been introduced in the aerospace industry, including canted winglets, blended winglets, split-scimitar winglets, spiroid winglets, wingtip fences, and

raked wingtips. Among these configurations, blended winglets are widely preferred for their smooth aerodynamic transition between the wing and winglet, which minimises interference drag and structural stress concentrations. Previous studies have demonstrated that winglets can improve aerodynamic efficiency by reducing vortex intensity and induced drag. Mostafa et al. [3] conducted a parametric investigation on spiroid winglets and reported significant reductions in wingtip vortex intensity compared to conventional wings. Other Computational Fluid Dynamics (CFD)-based investigations have also reported that blended winglets improve the lift-to-drag ratio and flight endurance across various aircraft configurations.

Although extensive studies have been conducted on winglet optimisation for commercial transport aircraft [4-7], limited research has focused on small and medium-sized UAV platforms, particularly involving combined aerodynamic and structural analyses. Existing studies mainly emphasise aerodynamic improvements while inadequately considering the structural integrity, material configuration, and failure behaviour of composite winglets under aerodynamic loading. Furthermore, limited information is available on the optimisation of cant-angle configurations for the ALUDRA-EE UAV platform. Since UAVs operate under different aerodynamic and structural constraints than large commercial aircraft, dedicated investigations are necessary to determine the most suitable winglet configuration to improve performance.

In addition to aerodynamic efficiency, structural reliability is also an important consideration in winglet design. Composite materials are increasingly used in aerospace structures due to their high strength-to-weight ratio, corrosion resistance, and fatigue performance. However, the structural response of the composite depends strongly on material selection, ply orientation, and structural configuration [8-9]. Therefore, both aerodynamic and structural performances must be evaluated simultaneously to ensure that the optimised winglet configuration can withstand operational loading conditions while maintaining lightweight characteristics.

Therefore, this study aims to investigate the aerodynamic and structural performance of blended composite winglets for the ALUDRA-EE UAV using CFD and finite element analysis. ALUNDRA-EE UAV was developed by Deftech Unmanned System Technology Sdn. Bhd is an extended-endurance version of the ALUDRA UAV developed by the same company. Three cant angle configurations, namely baseline wing without winglet, 45° blended winglet, and 60° blended winglet, are analysed using ANSYS Fluent to evaluate lift force, drag force, lift-to-drag ratio, and vortex intensity. These cant angles are chosen based on a study done by [10]. Subsequently, the best aerodynamic configuration is further analysed structurally using Abaqus software to evaluate the effects of composite material configuration and ply orientation on displacement, stress distribution, and failure indices. The outcome of this study is expected to contribute towards the development of more aerodynamically efficient and structurally reliable UAV winglet designs.

METHODOLOGY

Geometry and CAD Modelling

The wing and winglet geometries were developed using SolidWorks CAD software based on the ALUDRA-EE UAV wing configuration. The baseline wing used the RONCZ 1046 airfoil, which is commonly employed in UAV applications due to its favourable aerodynamic characteristics at low Reynolds numbers.

The geometric dimensions of the wing model are summarised in Table 1. The baseline wing consisted of a wingspan of 4765.32 mm and a chord length of 601.62 mm. To investigate the effect of winglets on aerodynamic performance, blended winglets were introduced at the wingtip region. The winglet height was selected as approximately 20% of the half-span length based on recommendations from previous winglet optimisation studies [2, 11, 12], which suggested that winglet extensions between 10% and 20% of the wingspan provide significant aerodynamic benefits while minimising additional structural weight.

Three wing configurations were analysed in this study: the baseline wing without a winglet, the wing with a 45° blended winglet, and the wing with a 60° blended winglet. A 75° canted-angle wing model was also simulated in a preliminary study, and it shows a decrease in the lift-to-drag ratio due to the transition from laminar to turbulent flow. Thus, it was not further considered in this study. The blended winglet geometry was selected due to its smoother transition between the wing and winglet, which reduces aerodynamic interference and stress concentration compared to conventional sharp-joint winglets. The cant angle was selected as the primary design variable because previous studies have shown that it

strongly influences wingtip vortex formation and induced drag characteristics.

Table 1: Geometrical Parameters of ALUDRA-EE Wing Model.

Parameter	Value
Airfoil Type	RONCZ 1046
Chord Length	601.62 mm
Wingspan	4765.32 mm
Half-span	2382.66 mm
Winglet Extension (20% wingspan)	461.90 mm

Computational Fluid Dynamics (CFD) Simulation

Computational Domain

The aerodynamic analysis was conducted using ANSYS Fluent software. The wing geometries generated in SolidWorks were imported into ANSYS Fluent for preprocessing and flow simulation. A rectangular computational domain was created to represent the airflow environment surrounding the wing model.

The enclosure dimensions were selected to replicate the dimensions of the Universiti Teknologi Malaysia (UTM) low-speed wind tunnel for potential future experimental validation. The computational domain dimensions were defined as Length (x-direction) = 6 m, Width (y-direction) = 2 m, and Height (z-direction) = 1.5 m. The wing model was positioned centrally within the domain to minimise boundary interference effects and ensure stable flow development around the wing.

Mesh Generation and Independence Study

A hybrid meshing strategy was employed to discretise the computational domain. Finer mesh elements were applied near the wing and winglet surfaces to accurately capture boundary layer development, pressure gradients, and wingtip vortex structures, while coarser mesh elements were applied in regions far from the wing to reduce computational cost.

Since different winglet geometries were investigated, the total number of elements varied slightly between configurations. A mesh independence study was conducted to ensure that the simulation results were independent of mesh size. Several mesh densities were tested until the variation in lift and drag coefficients became sufficiently small, as shown in Figure 1, the example of a mesh convergence study for a 60° blended winglet wing model.

The final mesh configuration was selected based on solution convergence and computational efficiency as presented in Table 2. Inflation layers were also applied near the wall surfaces to improve near-wall flow prediction.

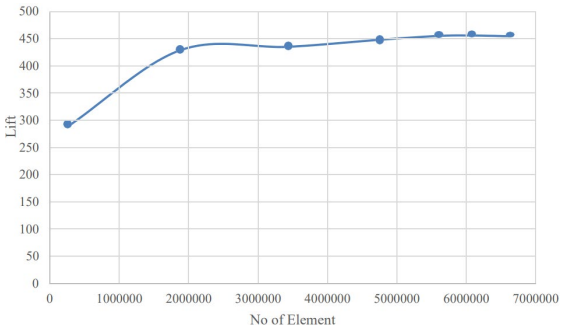

Figure 1: Example of mesh convergence study based on lift force (N) result for 60° blended winglet wing model.

Table 2: Mesh Information for Wing Configurations.

Wing Configuration	Mesh Size (m)		Number of Elements
Baseline	0.040		15,348,184
45° Winglet	0.061		6,557,718
60° Winglet	0.060		6,866,396

Boundary Conditions and Solver Settings

The CFD simulations were performed under steady-state incompressible flow conditions. Air was selected as the working fluid with standard atmospheric properties at 25°C. The inlet velocity was specified as 30.867 m/s in the x-direction, corresponding to the operating condition of the ALUDRA-EE UAV. The boundary conditions applied in the simulation are summarised as follows:

- Inlet velocity: 30.867 m/s
- Air temperature: 25°C
- Static pressure: 101.5 kPa
- Turbulence intensity: 5%
- Outlet pressure: 0 Pa gauge pressure
- Wall condition: No-slip wall

The Shear Stress Transport (SST) k-ω turbulence model was employed in this study due to its superior ability to predict flow separation, adverse pressure gradients, and wingtip vortex behaviour compared to standard k-ε models [13]. The SST k-ω model combines the advantages of the k-ω model near the wall and the k-ε model in the free-stream, making it suitable for aerodynamic simulations involving lifting surfaces.

The Lambda 2 Criterion is used to measure vortex intensity. The Lambda 2 Criterion is a vortex-core line detection algorithm that can reliably identify vortices in a three-dimensional fluid velocity field. The vortex is defined as the area in the flow field where the symmetric matrix $S^2 + \Omega^2$ contains two negative eigenvalues. S is the tension tensor, and Ω represents the vorticity tensor.

Wing Loading Analysis Using Schrenk Approximation

The spanwise lift distribution of the wing models was evaluated using the Schrenk approximation method. Schrenk's approximation is a classical aerodynamic method used to estimate the lift distribution along an untwisted wing by averaging the actual wing planform distribution with an equivalent elliptical lift distribution [14].

The local wing-loading distribution was analysed for both the baseline wing and the optimised winglet configuration to evaluate the influence of winglets on the aerodynamic load distribution. Lower wing loading generally improves take-off performance, reduces stall speed, and enhances manoeuvrability.

Structural Analysis Using Abaqus

The structural analysis of the optimised blended winglet configuration was conducted using SIMULIA Abaqus CAE software. Based on the CFD results, the 60° blended winglet configuration was selected for structural evaluation due to its superior aerodynamic performance. Two structural configurations were investigated: a hollow winglet with internal rib reinforcement and a solid winglet.

The objective of the structural analysis was to determine the most suitable composite material configuration and ply orientation that provides high structural stiffness, minimal displacement, and acceptable failure indices.

Material Configuration and Composite Layup

Three composite material configurations were investigated, which are E-glass composite, carbon fibre fabric, and unidirectional (UD) carbon composite

For the hollow winglet configuration, the structure consisted of composite skin layers and a Divinycell H45 foam core. Different ply orientations were also analysed to evaluate their influence on structural stiffness and stress distribution. The investigated ply orientations included [0°,0°,0°], [45°,0°,45°], and [-45°,0°,45°].

Boundary Conditions and Failure Analysis

The winglet root section was modelled using encastre boundary conditions, where all translational and rotational degrees of freedom were fully constrained to represent rigid attachment to the wing structure, as shown in Figure 2. Aerodynamic loading obtained from the CFD analysis was applied to the winglet surfaces. Tie constraints were applied between the winglet structure and internal ribs to represent adhesive bonding conditions. The structural performance was evaluated based on maximum displacement, Von Mises stress, Tsai-Hill failure index, Tsai-Wu failure index, and structural mass as studied in [8].

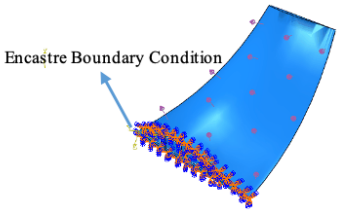

Figure 2: The applied boundary conditions for the structure failure analysis

A mesh independence study was also conducted to ensure numerical stability and accuracy of the structural simulation results, as shown in Figure 3. Composite failure indices lower than unity were considered structurally safe under the applied loading conditions.

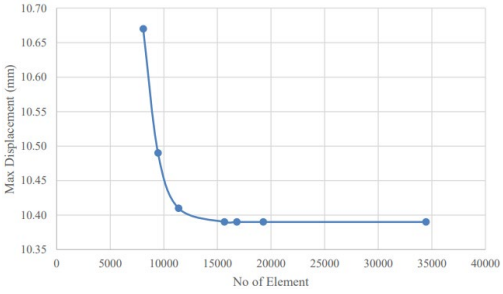

Figure 3: Mesh independency study based on the maximum displacement result

Results And Discussion

Aerodynamic Performance Analysis

The aerodynamic performance of the baseline wing and blended winglet configurations was

evaluated using CFD simulations in ANSYS Fluent. The analysed parameters included lift force, drag force, lift-to-drag ratio, and wingtip vortex intensity. The vortex behaviour near the wingtip was evaluated using the Lambda-2 criterion (Table 3), which is commonly used to identify coherent vortex structures in aerodynamic flows.

Table 3: Streamline plot for wing model.

Wing Model	Streamline Plot
Baseline wing	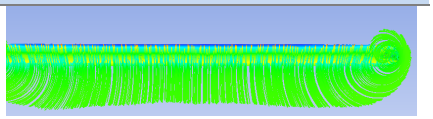 Lambda 2 Criterion: 169453 s^{-2}
Blended Winglet 45°	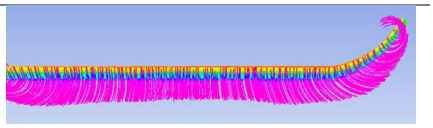 Lambda 2 Criterion: 33962.7 s^{-2}
Blended wing 60°	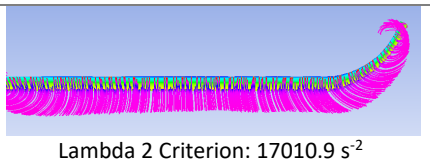 Lambda 2 Criterion: 17010.9 s^{-2}

Table 4: Summary of aerodynamic simulation results.

Wing Configuration	Lift (N)	Drag (N)	L/D Ratio
Baseline Wing	365.18	29.76	12.27
45° Blended Winglet	453.63	22.31	20.33
60° Blended Winglet	460.68	20.72	22.23

Based on Table 4, the results demonstrate that installing blended winglets significantly improved the aerodynamic performance of the ALUDRA-EE UAV. Compared to the baseline wing, both winglet configurations produced higher lift force and lower drag force, indicating improved aerodynamic efficiency due to the reduction of induced drag generated by wingtip vortices.

Among all configurations, the 60° blended winglet achieved the best aerodynamic performance with the highest lift force of 460.68 N and the lowest drag force of 20.72 N. Consequently, the lift-to-drag ratio increased substantially from 12.27 for the baseline wing to 22.23 for the 60° blended winglet configuration. This improvement indicates that the winglet effectively weakened the wingtip vortex strength and improved lift distribution along the wingspan. A similar trend was also reported by Madhanraj et in [10].

The Lambda-2 criterion results further support this observation. The baseline wing generated the strongest vortex structures near the wingtip region, while the 60° blended winglet produced the lowest vortex intensity. The reduction in vortex strength can be attributed to the upward deflection of airflow caused by the winglet, which reduced pressure equalisation between the upper and lower wing surfaces. Consequently, the induced drag was significantly reduced.

The aerodynamic improvements observed in this study are consistent with previous investigations of blended winglet performance [10], which reported that winglets improve the lift-to-drag ratio and reduce vortex intensity. The smoother aerodynamic transition between the wing and the blended winglet also minimised interference drag and improved overall flow behaviour around the wingtip.

Wingtip Vortex Behaviour

The streamline visualisations obtained from the CFD simulations (Table 3) revealed clear differences in vortex formation between the analysed wing configurations. The baseline wing exhibited strong rotational flow structures at the wingtip due to the direct interaction between the high-pressure lower surface and low-pressure upper surface airflow.

The introduction of blended winglets altered the wingtip flow structure by redirecting vortex formation away from the wingtips. The 45° winglet configuration reduced the vortex intensity considerably, while the 60° winglet configuration produced the smallest and weakest vortex structure among all cases. This behaviour indicates that larger cant angles are more effective at controlling spanwise airflow migration and suppressing induced drag.

The reduction in vortex intensity benefits not only aerodynamic efficiency but also wake turbulence reduction and improved flight stability during cruise conditions. These findings indicate that the winglet cant angle is a critical design parameter that affects aerodynamic performance.

Lift Coefficient Variation with Angle of Attack

The aerodynamic characteristics of the optimised 60° blended winglet configuration were further analysed at different angles of attack to determine its lift behaviour and stall characteristics, as shown in Figure 4. The results showed that the lift coefficient increased progressively as the angle of attack increased from 0° to 15°. The maximum lift

coefficient was achieved at approximately 15°, indicating the stall onset angle of the wing configuration. Beyond this angle, the lift coefficient began to decrease due to airflow separation occurring over the upper wing surface.

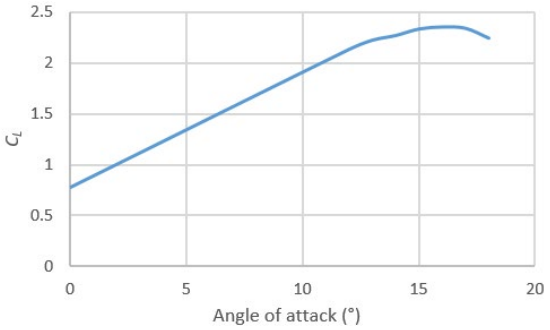

Figure 4: Lift coefficient of blended winglet 60° wing model at different angles of attack

At lower angles of attack, the airflow remained attached to the wing surface, resulting in stable lift generation and relatively low drag. As the angle of attack increased, the pressure difference between the upper and lower surfaces became larger, generating a higher lift force. However, an excessive angle of attack caused boundary-layer separation and increased flow instability, leading to aerodynamic stall.

The aerodynamic performance improvement achieved with the 60° blended winglet significantly enhanced the UAV's operational capability. The simulation results indicated that the UAV's range increased by approximately 26.14% and its flight endurance by approximately 41.7%. These improvements are particularly beneficial for UAV missions involving long-duration surveillance and reconnaissance operations.

Wing Loading Distribution

The wing loading distribution along the half-span of the wing was analysed using Schrenk's approximation method [14]. The comparison between the baseline wing and the optimised 60° blended winglet configuration presented in Figure 5 showed that both wing models experienced maximum lifting force near the wing root and minimum lifting force near the wingtip region.

However, the optimised blended winglet configuration exhibited lower overall wing loading compared to the baseline wing. The baseline wing recorded a peak local lifting force of approximately 2813.75 N/m, whereas the 60° blended winglet configuration reduced the peak value to approximately 2322.45 N/m.

The reduction in wing loading indicates that the winglet improved lift distribution along the wingspan and reduced aerodynamic stress concentration near the wing root region. Improved lift distribution contributes to better aerodynamic efficiency, lower stall speed, and enhanced flight stability.

Furthermore, lower wing loading generally leads to shorter take-off and landing distances, improved manoeuvrability, and reduced structural loading during flight operations. Therefore, the optimised winglet configuration not only enhanced aerodynamic efficiency but also improved flight handling characteristics.

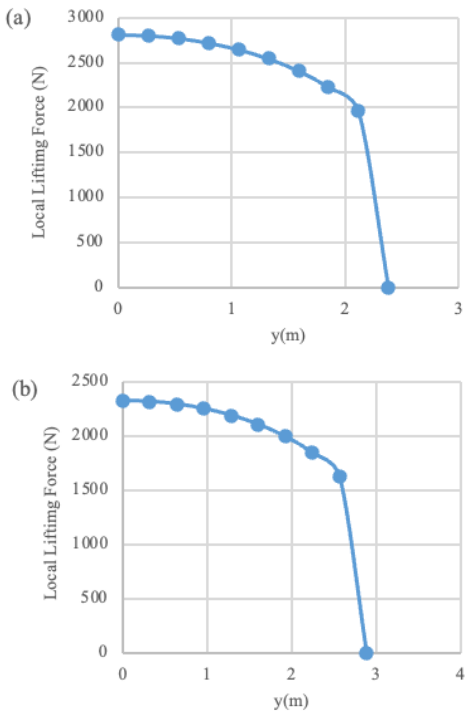

Figure 5: Wing loading distribution on half wingspan (a) Baseline wing model (b) Blended winglet 60° wing model

Structural Analysis of Composite Winglet

Following the aerodynamic optimisation study, the 60° blended winglet configuration was selected for structural analysis in Abaqus CAE. The structural investigation focused on evaluating the effects of composite material selection and ply orientation on displacement, stress distribution, and failure behaviour [8].

Hollow Winglet with Different Composite Materials

The first optimisation study investigated the structural behaviour of a hollow blended winglet reinforced with internal ribs using three different composite material configurations. The results of this investigation are tabulated in Table 5.

The results indicated that the carbon fibre fabric configuration exhibited the best structural performance among the investigated materials. Although the E-glass configuration produced slightly lower stress values, the carbon fibre fabric configuration achieved significantly lower displacement while maintaining lower structural mass.

The UD carbon configuration produced the highest displacement and stress values, indicating lower structural stiffness under aerodynamic loading. Nevertheless, all configurations recorded Tsai-Hill and Tsai-Wu failure indices below unity, indicating that the winglet structures remained structurally safe under the applied loading conditions.

The superior performance of the carbon fibre configuration can be attributed to its higher stiffness-to-weight ratio compared to E-glass and UD carbon materials. Therefore, the carbon fibre fabric configuration was selected for further optimisation of ply orientation.

Table 5: Structural performance of hollow winglet configurations.

Material Configuration	Mass (kg)	Max Displacement (mm)	Stress (MPa)	Tsai-Hill	Tsai-Wu
E-Glass	1.192	9.886	30.82	0.1542	0.1521
Carbon Fibre Fabric	1.043	6.882	32.17	0.1412	0.1408
UD Carbon	1.043	11.33	43.66	0.3579	0.3759

Table 6: Structural performance for different ply orientations.

Ply Orientation	Mass (kg)	Max Displacement (mm)	Von Mises Stress (MPa)	Tsai-Hill	Tsai-Wu
[0°,0°,0°]	1.043	6.882	32.17	0.1412	0.1408
[45°,0°,45°]	1.043	6.195	61.05	0.1594	0.1577
[-45°,0°,45°]	1.043	6.316	65.06	0.1632	0.1790

Table 7: Structural performance of solid winglet configurations.

Material Configuration	Mass (kg)	Max Displacement (mm)	Von Mises Stress (MPa)	Tsai-Hill	Tsai-Wu
E-Glass	1.590	2.889	12.40	0.0374	0.0385
Carbon Fibre Fabric	1.452	1.656	12.95	0.0321	0.0325
UD Carbon	1.452	4.861	54.66	0.1868	0.1862

Effect of Ply Orientation on Hollow Winglet Performance

The influence of composite ply orientation on structural behaviour was subsequently investigated using the carbon fibre fabric configuration.

Table 6 shows that the [45°,0°,45°] ply orientation produced the lowest displacement among all configurations, indicating improved torsional stiffness and better load distribution. Although the Von Mises stress increased compared to the [0°,0°,0°] configuration, the failure indices remained below unity, confirming structural safety.

The improved performance of angled ply orientations is mainly due to their enhanced resistance to multidirectional loading conditions induced by aerodynamic forces acting on the winglet structure. Consequently, the [45°,0°,45°] orientation was selected as the optimal ply configuration for the hollow winglet design.

Solid Winglet Structural Performance

The second optimisation study investigated the structural behaviour of solid winglet configurations using different composite materials. The result of this optimisation is presented in Table 7.

The solid winglet configurations demonstrated significantly improved structural performance

compared to the hollow winglet designs. Among all configurations, the carbon fibre fabric model achieved the lowest displacement value of 1.656 mm while maintaining relatively low stress and failure indices.

Although the E-glass configuration exhibited slightly lower stress values, its higher structural mass made it less attractive for UAV applications where lightweight structures are preferred. The UD carbon configuration again produced the highest stress and displacement values due to its lower stiffness characteristics.

The improved stiffness observed in the solid winglet configuration can be attributed to increased structural continuity and greater effective load-carrying capacity. Abaqus simulations also indicated that the solid carbon fibre winglet possessed a higher effective Young's modulus compared to the hollow configuration.

Conclusion

This study investigated the aerodynamic and structural performance of blended composite winglets for the ALUDRA-EE UAV using CFD and finite element analysis. Three wing configurations consisting of a baseline wing, 45° blended winglet, and 60° blended winglet were analysed to evaluate the influence of winglet cant angle on aerodynamic efficiency and structural behaviour.

The CFD simulation results showed that installing blended winglets significantly improved the UAV's aerodynamic performance compared to the baseline wing configuration. Among the investigated configurations, the 60° blended winglet achieved the best aerodynamic performance, producing the highest lift and the lowest drag. Consequently, the lift-to-drag ratio improved substantially from 12.27 for the baseline wing to 22.23 for the optimised winglet configuration. The streamline and Lambda-2 criterion analyses further revealed that the 60° blended winglet effectively weakened wingtip vortex formation and reduced induced drag by controlling spanwise airflow migration near the wingtip region.

The aerodynamic performance evaluation at different angles of attack showed that the optimised winglet configuration improved aerodynamic efficiency, resulting in significant operational improvements: the estimated UAV range and endurance increased by approximately 26.14% and 41.7%, respectively. In addition, the wing loading analysis indicated that the optimised blended winglet produced a more favourable lift distribution along the wingspan and reduced peak local wing loading compared to the baseline wing.

Structural analyses conducted with Abaqus demonstrated that all investigated composite winglet configurations met the structural safety requirement. Among the analysed materials, the carbon fibre fabric consistently exhibited superior structural performance due to its high stiffness-to-weight ratio. For the hollow winglet configuration, the [45°,0°,45°] ply orientation produced the lowest displacement and improved load distribution capability under aerodynamic loading conditions. Comparative analysis of hollow and solid winglet configurations further revealed that the solid composite winglet exhibited significantly greater structural stiffness and lower displacement while maintaining acceptable stress and failure indices.

Overall, the results of this study demonstrate that the integration of blended winglets can significantly enhance both aerodynamic efficiency and structural reliability of UAV platforms. The combined CFD and finite element approach adopted in this research also provides a systematic framework for future UAV winglet optimisation studies that involve both aerodynamic and composite structural considerations.

For future work, additional geometric parameters such as sweep angle, toe angle, taper ratio, and winglet height may be investigated to further improve aerodynamic performance. Experimental validation through wind-tunnel testing and structural testing is also recommended to confirm the numerical findings presented in this study.

Acknowledgements

The authors would like to express their gratitude to Deftech UST for supporting this research project and providing valuable insights and expertise that greatly assisted the research.

References

[1] Tajuddin, N., Mat, S., Said, M. and Mansor, S., 2017. Flow Characteristic of Blunt-Edged Delta Wing at High Angle of Attack. Journal of Advanced Research in Fluid Mechanics and Thermal Sciences. 39: 17–25.

[2] Whitcomb, R. T., 1976. A Design Approach and Selected Wind-Tunnel Results at High Subsonic Speeds for Wing-Tip Mounted Winglets. Hampton, Virginia: NASA Langley Research Center, NASA Technical Note D-8260.

[3] Mostafa, S., Bose, S., Nair, A., Raheem, M. A., Majeed, T., Mohammed, A. and Kim, Y., 2014. A Parametric Investigation of Non-Circular Spiroid Winglets. EPJ Web of Conferences. 67: 02077.

[4] Lishifelshyal, W., 2016. Analysis of Drag over a Wing Model with and without Raked Wingtip. EPRA International Journal of Research and Development. 1(4): 65–70.

[5] Guerrero, J. E., Sanguineti, M. and Wittkowski, K., 2020. Variable Cant Angle Winglets for Improvement of Aircraft Flight Performance. Meccanica. 55(10): 1917–1947.

[6] Gueraiche, D. and Popov, S., 2017. Winglet Geometry Impact on DLR-F4 Aerodynamics and an Analysis of a Hyperbolic Winglet Concept. Aerospace. 4(4): 60.

[7] Padmanathan, P., Aswin, S., Satheesh, A., Kanna, P. R., Palani, K., Devi, N. R., Sobota, T., Taler, D., Taler, J. and Węglowski, B., 2024. Parametric Optimization Study of Novel Winglets for Transonic Aircraft Wings. Applied Sciences. 14(17): 7483.

[8] Israr, H. A., Chwen, T. S., Latif, A. A., Wong, K. J., Koloor, S. S. R., Yidris, N. and Yahya, M. Y., 2022. Preliminary Structural Design of Coreless Spoiler by Topological Optimization. Processes. 10: 2076.

[9] Naufal, M. I., Wong, K. J., Israr, H. A., Nejad, A. F., Koloor, S. S. R., Gan, K. W., Faizi, M. K. and Siebert, G., 2024. Digital Image Correlation Technique for Failure and Crack Propagation of Fibre-Reinforced Polymer Composites—A Review. Composites and Advanced Materials. 33:1-23.

[10] Madhanraj, V., Chandra, K. G., Swprazeeth, D. and Gopal, B. D., 2021. Design and Computational Analysis of Winglets. Turkish Journal of Computer and Mathematics Education. 12(7): 1–9.

[11] Torenbeek, E., 2013. Advanced Aircraft Design: Conceptual Design, Analysis and Optimization of Subsonic Civil Airplanes. Chichester: Wiley.

[12] NATO Advisory Group for Aerospace Research and Development, 1985. Aircraft Drag Prediction and Reduction. AGARD Report No. 723.

[13] Chmielewski, M. and Gieras, M., 2013. Three-Zonal Wall Function for k-ε Turbulence Models. Computational Methods in Science and Technology. 19(2): 107–114.

[14] Schrenk, O., 1941. A Simple Approximation Method for Obtaining the Spanwise Lift Distribution. The Journal of the Royal Aeronautical Society. 45(370): 331–336.

.